

## Military Application of Differential FTIR Radiometry for Passive Standoff Detection

Jean-Marc Thériault, Eldon Puckrin, Hugo Lavoie,  
Francois Bouffard and Denis Dubé

Defence Research and Development Canada – Valcartier  
2459, Boulevard Pie-XI N., Val-Bélair, Québec, G3J 1X5  
CANADA

[jean-marc.theriault@drdc-rddc.gc.ca](mailto:jean-marc.theriault@drdc-rddc.gc.ca) / [eldon.puckrin@drdc-rddc.gc.ca](mailto:eldon.puckrin@drdc-rddc.gc.ca)

### ABSTRACT

For the past six years Defence R&D Canada – Valcartier has been developing a method for the passive remote sensing of chemical vapours by differential Fourier-transform infrared (FTIR) radiometry. The originality of the method lies in the use of a double-input beam FTIR spectrometer (CATSI) optimized for optical subtraction. This configuration automatically reduces the clutter-to-signal ratio and permits real-time monitoring of chemical agents. The passive standoff results obtained with the CATSI instrument at several major open-air field trials have shown that the system can successfully detect, identify and quantify a number of chemical vapours at various distances. In particular, the detection method has been used at short range (105 m) to map the column amounts of ammonia, methanol and several binary mixtures with consistent results. At medium range (1.5 km), the measurement technique has been successfully used to detect and identify low, medium and high concentrations of vapour mixtures of DMMP and SF<sub>6</sub> but appears to have limited quantification capabilities in its original form. At long range, CATSI has successfully measured SF<sub>6</sub> gas amounts at a standoff distance of 5.7 km at DRDC Valcartier. Many of the measurements have been made for complex mixtures of gases exhibiting a strong overlap of spectral bands. In addition, the CATSI sensor has been applied to the problem of passively detecting bio-aerosols at ranges of up to 3 km. The instrument has also been shown to demonstrate some capability in detecting and identifying liquid CW contaminants on surfaces at standoff distances of up to 60 m. Very recently, the CATSI system has been employed to detect, identify and quantify classical CW agents and their simulants in an open-air field trial. An initial effort in adapting the orthogonal background suppression (OBS) technique to the differential detection method has been undertaken with some success. The application of the OBS technique has been applied to differential radiance spectra of DMMP at a standoff distance of 500 m. All these experiments clearly show the relevance of the differential detection technique for on-line monitoring and surveillance of toxic chemical agents.

### 1.0 INTRODUCTION

The military of modern Defense organizations are using a variety of electro-optical systems for the remote sensing of target characterization. The development of passive IR spectral sensors has grown to a point at which it is now considered a vital technology for the remote monitoring of battlefield environments, providing unique information concerning ongoing maneuvers. One of the most promising applications in surveillance is the passive standoff detection of chemical warfare agents and toxic vapours by Fourier-transform infrared (FTIR) radiometry (e.g. Refs. 1,2). In NATO countries, there is a growing need for fieldable, rapid-response surveillance systems that provide timely and accurate chemical threat assessments, thus ensuring prompt avoidance and deployment of countermeasures.

Thériault, J.-M.; Puckrin, E.; Lavoie, H.; Bouffard, F.; Dubé, D. (2005) Military Application of Differential FTIR Radiometry for Passive Standoff Detection. In *Emerging EO Phenomenology* (pp. 23-1 – 23-12). Meeting Proceedings RTO-MP-SET-094, Paper 23. Neuilly-sur-Seine, France: RTO. Available from: <http://www.rto.nato.int/abstracts.asp>.

## Military Application of Differential FTIR Radiometry for Passive Standoff Detection

---

Defence R&D Canada – Valcartier (DRDC Valcartier) has been developing a method for the passive standoff detection and identification of chemical vapours by differential FTIR (Fourier-transform infrared) radiometry. The method is based on the use of a double-input beam FTIR interferometer referred to as CATSI (Compact ATmospheric Sounding Interferometer [3, 4]). The differential detection capability of CATSI provides two unique features for a field-deployable instrument. First, CATSI maintains a constant calibration, thereby providing reliable quantitative measurements over a long period of time. Second, it can perform the real-time optical subtraction of the background signal from the target signal yielding a target signature minimally perturbed by the background radiation.

The purpose of this paper is to summarize the main experimental results obtained throughout the development of the CATSI project in order to demonstrate the capability of the CATSI sensor for the passive remote sensing of chemical threats. First, a description of the CATSI sensor and its associated detection algorithm (GASEM) is presented. This is followed by trial results for the passive standoff detection of chemicals at short, medium and long ranges. Two additional investigations for the passive standoff detection of surface contaminants and bio-aerosols are also described. Finally, initial results obtained with a newly developed background suppression algorithm applied to CATSI data is presented. The overall analysis emphasizes the military application of differential FTIR radiometry for passive standoff detection of chemical vapour threats.

### 2.0 CATSI SENSOR

The passive standoff detection approach using the CATSI system takes advantage of the differential detection capability provided by an optimized dual-beam interferometer with adjacent fields-of-view [3, 4]. In this system two beams of thermal radiation originating from different scenes can be optically combined onto a single detector and subtracted in real-time. Thus, if one beam entering the interferometer corresponds to the target-cloud-plus-background scene and the other corresponds to a consistent background scene, then the resulting differential spectrum corresponds primarily to the target-cloud scene minimally perturbed by the background. The standard configuration for the CATSI sensor consists of two identical Newtonian telescopes (Fig. 1A), each with a diameter of 10 cm, which are optically coupled to the dual-beam interferometer. Each telescope can be individually aimed at a selected scene, i.e., one on the target cloud scene and the other on a cloud-free background scene. This system allows measurements of spectra to be made according to the following specifications: (1) scene field-of-view (FOV) of 11 mrad or less, (2) spectral coverage from 7 to 14  $\mu\text{m}$ , and (3) a maximum spectral resolution of 1  $\text{cm}^{-1}$ . Coarse and fine adjustments in the azimuth and elevation pointing directions are simply achieved by rotating the whole assembly, which is mounted on a tripod. Additional information on the standard CATSI instrument and its radiometric calibration has been reported elsewhere [3].

For experiments with high sensitivity requirements, a modified configuration of the CATSI sensor was implemented. A picture of the modified sensor is shown in Fig. 1B. In this case a single 25-cm diameter Cassegrain telescope is used to replace the two smaller telescopes. The scene FOV at the focus of the telescope is split into two equal parts by a 45-degree reflecting prism. The resulting two input beams are optically subtracted by the interferometer. The advantage of the 25-cm telescope configuration is to improve the sensitivity by a factor of 6 for a given FOV. The combination of the 25-cm telescope with the interferometer optics yields a detector FOV of approximately 3.5 mrad. The drawback of this configuration is that the angular separation of the two selected scenes remains constant, as opposed to the case of the 10-cm telescope configuration. As discussed below the 10-cm telescope configuration was mainly used for chemical vapour detection and the 25-cm telescope configuration was used for bio-aerosol detection.

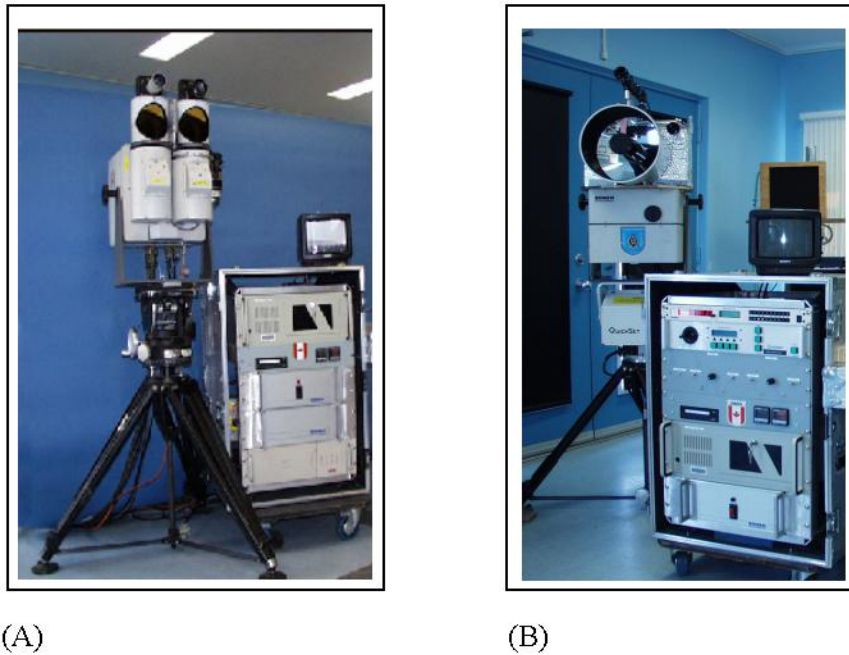


Figure 1: Photos of the CATSI system. (A) Represents the system with the 10-cm telescope configuration and (B) represents the system with the 25-cm telescope configuration

### 3.0 DIFFERENTIAL DETECTION METHOD AND ALGORITHM

The passive standoff monitoring of chemical vapours is based on the differential detection equation derived with the atmospheric parameters defined in Fig. 2A. It can be verified [5] that if the vapour cloud occupies a fraction  $f$  of the field-of-view then the radiance differential would be given by,

$$\delta L_{calc} \equiv L_{gas} - L_{clear} = \Delta L_{clear} + f(1 - \tau_{gas})(B_{gas}\tau_{near} + N_{near} - L_{clear} - \Delta L_{clear}). \quad (1)$$

Equation 1 represents a general expression that gives the differential radiance of a vapour cloud having a filling factor ( $f$ ) with a provision for handling a possible background variation ( $\Delta L_{clear}$ ) between the two simultaneously observed scenes. The parameter  $L_{gas}$  is the radiance of an atmosphere containing the vapour cloud where  $B_{gas}$  and  $\tau_{gas}$  represent the Planck radiance and transmittance, respectively, associated with the vapour cloud,  $(1 - \tau_{gas})$  denotes the vapour cloud spectral emissivity, and  $N_{near}$  corresponds to the near-field path radiance. For the general case of a gas mixture composed of  $i$  compounds,  $\tau_{gas}$  is given by,

$$\tau_{gas} = \exp\left[-\sum_i \alpha_i(\nu)C_iL\right], \quad (2)$$

where  $\alpha_i(\nu)$  is the spectrally dependent absorption coefficient (1/ppm-m) of compound  $i$ ,  $C_i$  is the volume concentration (ppmv) of compound  $i$ ,  $L$  is the length (m) of the cloud sample, and  $\nu$  is the wavenumber ( $\text{cm}^{-1}$ ). Note that the quantity of interest,  $C_iL$ , is given here in ppm-m.

The basic processing strategy of the detection algorithm (GASEM – GASEous Emission Monitoring, see Ref. 6) consists of adjusting a set of gas parameters (e.g.,  $CL$  and temperature) to generate a calculated

**Military Application of Differential FTIR Radiometry for Passive Standoff Detection**

spectrum ( $\delta L_{calc}$ ) that best fits the spectral features of the measured differential spectrum ( $\delta L_{meas}$ ) inside a spectral band from  $\nu_{min}$  to  $\nu_{max}$ . The minimization equation can be written as,

$$\min \sum_{\nu_{min}}^{\nu_{max}} (\delta L_{calc} - \delta L_{meas})^2 . \tag{3}$$

Note that the background radiance drift between the two scenes ( $\Delta L_{clear}$ ) is handled by including a blackbody temperature variation ( $\Delta\theta$ ) in the fitting process. In the current version of GASEM, the radiance differential,  $\delta L_{calc}$ , is calculated using Eq. 2 with  $\alpha_i(\nu)$  taken from an IR spectral database. A fast atmospheric transmission/emission model has been integrated into GASEM. This model is a look-up table version of the MODTRAN model [7].

The detection and identification of a given chemical is achieved when the chemical cloud parameters retrieved through a SIMPLEX minimization are physically acceptable, and when a proper correlation factor between the measured spectrum and the spectrum calculated with the best-fit parameters is obtained. The correlation factor ( $r^2$ ) is defined here as the square of the Pearson's correlation coefficient. It is given by,

$$r^2 = \frac{\left( \sum_{i=1}^{n_{chan}} (x_i - \bar{x})(y_i - \bar{y}) \right)^2}{\sum_{i=1}^{n_{chan}} (x_i - \bar{x})^2 \cdot \sum_{i=1}^{n_{chan}} (y_i - \bar{y})^2} , \tag{4}$$

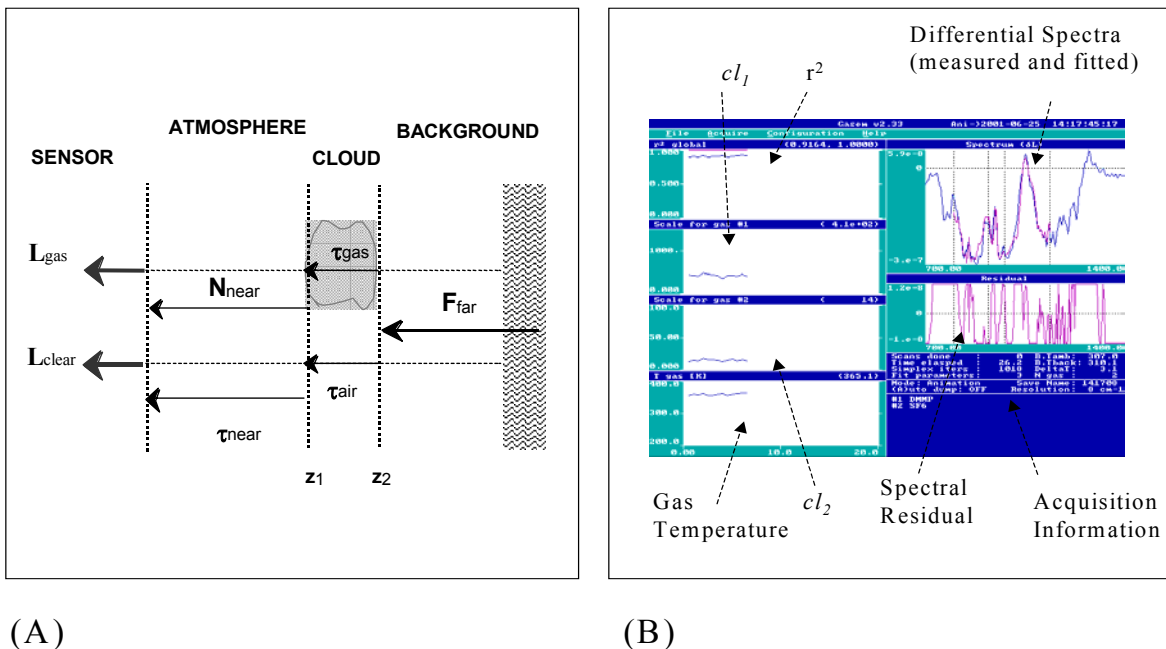


**Figure 2: (A) Diagram and the terminology defining the geometry for the differential detection with a dual beam interferometer, and (B) a typical screen output produced by the GASEM software during acquisition**

with  $x_i \equiv \delta L_{calc}$ ,  $y_i \equiv \delta L_{meas}$ , and where  $n_{chan}$  represents the number of spectral channels of the chosen band for the spectral fit,  $x_i$  is equal to the spectral radiance differential calculated with the best-fit parameters plus the background temperature drift,  $\Delta\theta$ , and  $y_i$  is equal to the measured spectral radiance differential. The terms  $\bar{x}$  and  $\bar{y}$  represent the average over the spectral band of the calculated and the measured radiance differentials, respectively. This correlation factor, which varies from no correlation ( $r^2 = 0$ ) to perfect correlation ( $r^2 = 1$ ), is then used to make a decision on the presence or the absence of a given chemical cloud. Figure 2B shows a typical picture of the output screen with the associated parameters generated with the GASEM software during an acquisition at a spectral resolution of  $8 \text{ cm}^{-1}$ .

## 4.0 FIELD MEASUREMENT RESULTS AND ANALYSIS

Results are presented from several trials that demonstrate the passive standoff detection capability of the CATSI sensor in measuring a variety of chemical targets at several distances. The types of targets include chemical plumes, both single gases and binary mixtures, at standoff distances of up to 5.7 km, chemical warfare agents on surfaces and bio-aerosols at distances of up to 3 km.

### 4.1 Measurement of Chemical Plumes

The differential detection method has been tested for several chemical vapours over distances of several hundred metres during open-air experiments held at DRDC Valcartier and Ft. Riley, Kansas (Sept. 1998). In particular, the detection method has been used to probe the concentration (column amount) and the temperature of several vapour plumes at a distance of 105 m (Ft. Riley Trial). The temperature of the stack (plume generator built by AeroSurvey, see Ref. 8) was approximately constant at  $200 \text{ }^\circ\text{C}$  and for each release the flow rate was kept constant. The GASEM retrievals were performed using three variables; gas column amount ( $CL$ ), gas temperature ( $T_{gas}$ ), and an offset parameter. Other parameters including the ambient air temperature and humidity were obtained from on-site meteorological measurements. Figure 3 gives an example of a remote sensing result obtained for an ammonia plume where the measured differential radiance is compared to the one calculated by GASEM using the best fit column amount and temperature. For this measurement the field-of-view (FOV) of the scene telescope of CATSI was looking at position-2 (Fig. 3A) and the reference telescope was looking at the plume-free sky background (not shown on the picture). The CATSI sensor was operated at an apodized (cosine) resolution of  $4 \text{ cm}^{-1}$  with a FOV of 7 mrad and a co-adding time of approximately one second. As shown in Fig. 3B, the optical subtraction performed by the CATSI sensor yielded an ammonia plume spectrum almost free of background emission features from atmospheric interferants. The consistency of column amount retrievals obtained for ammonia, methanol and several binary mixtures probed at 105 m has demonstrated the capabilities of the GASEM algorithm and the relevance of the differential detection approach at short range [6].

To evaluate the technique at a medium range, we have selected a dataset recorded in a field trial held at the Nevada Test Site (NTS), June 2001. These results focus on the CATSI measurements of vapour plume mixtures of DMMP and  $\text{SF}_6$  probed at a distance of 1.5 km. The NTS stack height was 15.3 m and the diameter of the stack was approximately 72 cm. At this distance the FOV of the CATSI sensor was quite large compared to the plume diameter. In these conditions the fraction of the plume (filling factor) covering the FOV was estimated to be  $f = 0.035$ . There was a mountain in the background approximately 6 km behind the stack. The stack temperature was kept constant at approximately  $175 \text{ }^\circ\text{C}$ . For each release of the DMMP- $\text{SF}_6$  mixture the flow rate of the individual species was independently adjusted to generate various mixing ratios. Meteorological conditions were slightly variable with a temperature of  $31 - 33^\circ\text{C}$ , a wind speed of  $5 - 8 \text{ m/s}$ , and a relative humidity of  $15 - 20\%$ .



## Military Application of Differential FTIR Radiometry for Passive Standoff Detection

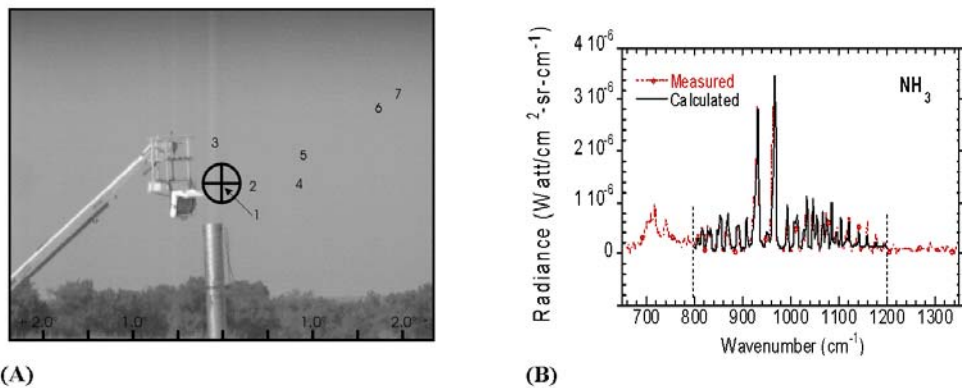


**Figure 3: (A) Photo of the plume generator seen with the seven locations across the plume monitored with the CATSI sensor; (B) Example of the spectral fit by GASEM obtained for one location on the ammonia plume**

Truthing data were not available for our analysis; however, since the concentrations (ppmv) of individual constituents were known precisely from the flow rates, it was possible to establish an estimate of the reference column density ( $CL$ ). The reference estimates,  $CL_{ref}$ , used in our analysis were obtained by computing the average  $CL$  of a cylinder-shaped plume that matched the shape and the size of the stack. No attempt was made to obtain a reference estimate of the plume temperature. For this analysis, GASEM was utilized to provide a best fit of the plume temperature using the  $CL$  reference estimates as inputs for the calculation. All of the GASEM calculations were performed with a plume filling factor of  $f = 0.035$ , and with the absorption coefficients of DMMP and  $SF_6$  that appear in Fig. 4A. The measurements were taken at a resolution of  $8\text{ cm}^{-1}$ . The spectral bands chosen for the fit were  $920 - 980\text{ cm}^{-1}$  for  $SF_6$  and  $800 - 1140\text{ cm}^{-1}$  for DMMP. Figure 4B shows a comparison between the measured and GASEM best-fit spectra obtained for a high DMMP concentration in the released mixture. In Fig. 4B, the best-fit spectrum was obtained by using the  $CL$  reference estimates of DMMP (1019 ppm-m) and  $SF_6$  (56 ppm-m) as inputs for the GASEM model, and using the plume temperature ( $T_{FIT}$ ) and the background temperature drift term ( $\Delta\theta$ ) as the two fitting parameters. In this case the fitted plume temperature was  $T_{FIT} = 351.6\text{ K}$  and  $\Delta\theta = -1.8\text{ K}$  (not indicated in the figure). The effect of the negative background temperature drift ( $\Delta\theta$ ) is to smoothly shift the spectra toward negative values. As observed, the best-fit spectrum reproduces relatively well the measured spectra with a correlation factor of  $r^2 = 0.859$ . The consistency of the results obtained for DMMP- $SF_6$  vapour mixtures demonstrated the detection and identification capabilities of the GASEM-CATSI approach for a standoff detection range of 1.5 km. A more complete analysis of results obtained at the NTS trial can be found in Ref. 5.

In an experiment to evaluate the technique for a long standoff distance of 5.7 km, we have used  $SF_6$  as a simulant target gas. This experiment was performed at the 5.7 km propagation range of DRDC Valcartier. To obtain a relatively uniform vapour cloud, the stabilized vapour release from an  $SF_6$  tank was connected to an aluminum pipe with a diameter of 4 cm and a length of 3 m. The pipe was mounted vertically on the roof of the source-site building. The top of the pipe was blocked and a series of 5-mm diameter holes were linearly distributed at 10-cm intervals along the pipe to act as point sources. This arrangement provided an extended linear source (3 m) of vapour as opposed to the punctual release directly available from the tank outlet. A regulator was used to stabilize the  $SF_6$  flow rate at values ranging from 20 to 200 L/min. For this experiment the 25-cm telescope configuration (Fig.1B) provided a FOV of approximately 20 meters at 5.7 km. With this configuration the two scenes simultaneously observed and optically subtracted ( $SF_6$  scene minus reference scene) by CATSI were separated by a distance of approximately 60 m. The basic experiment consisted of a continuous monitoring of  $SF_6$  released at a flow rate of 100 L/min for a period of one min. Figure 5A represents a sample of the differential spectral radiance measured (blue) with CATSI together with the GASEM best-fit calculation

(red). In this case, the correlation coefficient ( $r^2$ ) between the measured and the best-fit spectra is greater than 0.9 indicating very good agreement, and the estimated column density was approximately 14 ppm-m. This measurement (7 November 2002) was performed under clear sky conditions with an ambient air temperature of  $-5\text{ }^\circ\text{C}$  and a crosswind speed of approximately 2 - 5 m/s. The radiative contrast between the background scene, which consisted primarily of forest, and the vapour was estimated to be  $0.3\text{ }^\circ\text{C}$ . Figure 5B reports the correlation coefficient calculated for the overall monitoring period of two minutes. We see that the  $r^2$  is maximum (0.9) for approximately 45 s of the release period from 16:06:45 to 16:07:30. The increasing and decreasing wings of the  $r^2$  curve are simply related to the transit time required for the vapour cloud to move into and out of the scene field of view. A more extensive analysis of results obtained for a standoff distance of 5.7 km is presented in Ref. 9.

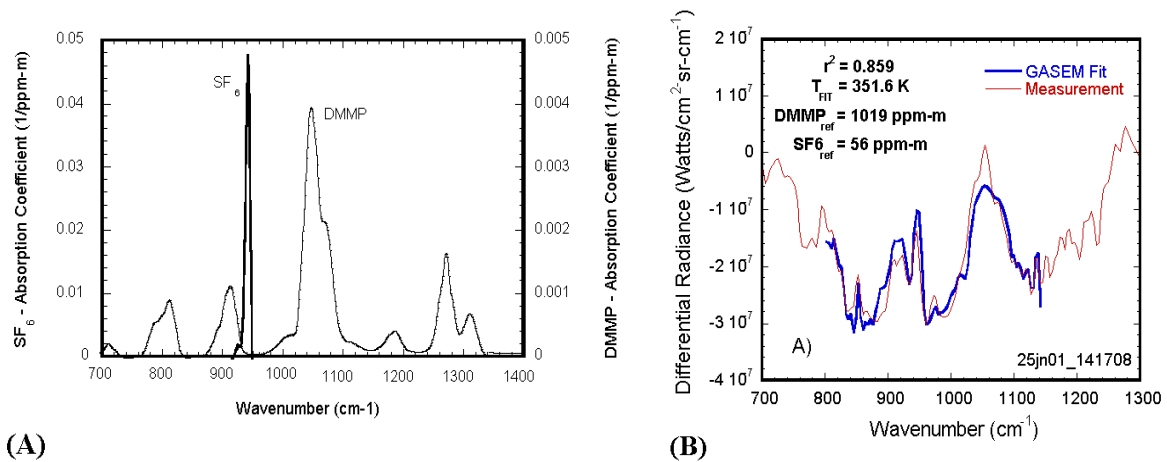


Figure 4: (A) Absorption coefficients of DMMP and SF<sub>6</sub>, and (B) the measured and computed best-fit spectra for a high DMMP mixture concentration.

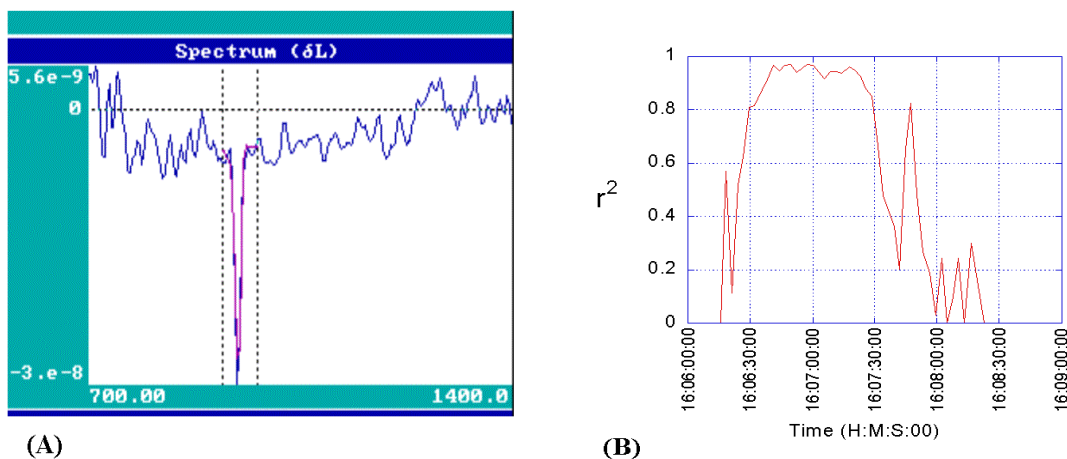
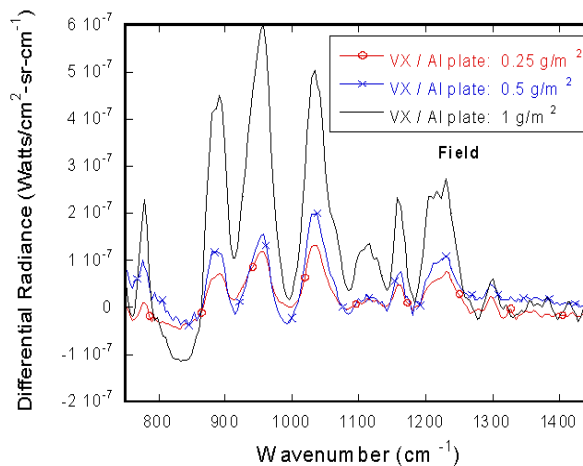


Figure 5: (A) Differential spectral radiance of SF<sub>6</sub> release measured with the CATSI sensor at a distance of 5.7 km, and (B) the  $r^2$  function of time.

## Military Application of Differential FTIR Radiometry for Passive Standoff Detection

### 4.2 Measurement of CW Agents on Surfaces

During the development of the CATSI project a significant effort was spent to investigate the passive standoff detection of liquid agent contaminants on surfaces. The measurement phase of this work was mainly performed during a field trial held at DRDC Suffield, Canada in September 2002. The goal of this trial was to verify that passive long-wave infrared spectrometric sensors have the potential to remotely detect surfaces contaminated with CW agents. The agents were applied to high-reflectivity surfaces of aluminum, low-reflectivity surfaces of Mylar, and several other materials. Figure 6 shows an example of differential radiances measured in the field at a standoff distance of 60 m with the CATSI sensor for three VX coverages (0.25, 0.5 and 1 g/m<sup>2</sup>) deposited on an aluminum plate. The results of this study [10] indicate that liquid contaminant agents deposited on high-reflectivity surfaces can be detected, identified and possibly quantified with passive sensors. For low-reflectivity surfaces, the presence of contaminants can usually be detected; however, their identification based on simple correlations with the absorption spectrum of the pure contaminant is not possible.



**Figure 6: Surface contaminant detection: differential radiance measured in the field at a standoff distance of ~ 60 m with the CATSI sensor for three VX coverages (0.25, 0.5 and 1 g/m<sup>2</sup>) deposited on an aluminum plate.**

### 4.3 Measurement of Bio-Aerosols

A significant effort was also undertaken to investigate the passive standoff detection of bio-aerosols. The excursion phase of the Technology Readiness Evaluation (TRE) trial (Dugway Proving Ground, USA, July 2002) enabled us to determine the capability of our differential passive standoff technique for measuring *Bacillus subtilis* (BG) clouds. For each BG release episode, the line-of-sight of the CATSI sensor was aimed at the cloud release scene. In this case, the 25-cm telescope configuration was used to narrow the FOV of the measurement scene. The elevation angle of the CATSI line-of-sight was fixed at approximately 0.2 - 0.3 degrees above the horizon in order to avoid the background terrain effect. The CATSI sensor was operated at a spectral resolution of 8 cm<sup>-1</sup> during the entire trial yielding a noise equivalent spectral radiance (NESR) of approximately 2x10<sup>-9</sup> W/cm<sup>2</sup> sr cm<sup>-1</sup>. Figure 7 shows an example of the detection and identification of a BG cloud at a distance of 3 km as measured with the CATSI instrument. The blue curve corresponds to the measurement and the red curve represents the corresponding GASEM best-fit spectrum. The bottom curve (black) in Fig. 7 corresponds to a measured spectrum without BG present, i.e. recorded prior to the BG release. The high value of the correlation



coefficient (0.79) indicates the presence of BG. Our analysis of three similar trial episodes confirms that BG clouds have been detected passively at a distance of 3 km for near-horizontal path scenarios (see Ref. 11). For these scenarios it has been found that the low thermal contrast between the BG cloud and the background yields weak but observable spectral signatures. However, the level of error associated with the *CL* estimate, which is related to the cloud temperature uncertainties, can be as large as a factor of five.

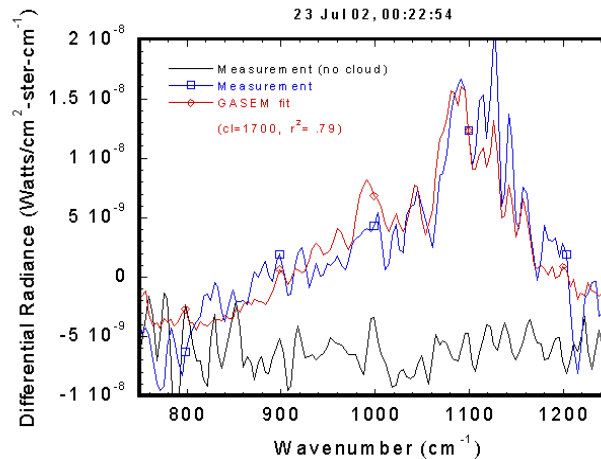


Figure 7: Bio-aerosol detection: example of a spectral measurement (blue curve) of a BG cloud made at a distance of approximately 3 km together with the corresponding GASEM best-fit spectrum (red curve). The bottom curve corresponds to a measured spectrum without BG.

## 5.0 DETECTION ALGORITHM DEVELOPMENT

The passive standoff detection of chemical vapours by differential FTIR radiometry (CATSI) works extremely well for relatively uniform backgrounds. However when the background behind the chemical vapour cloud is significantly different from the reference background the simple background drift correction implemented in the current GASEM algorithm (Sec. 3) may be inefficient. A typical example of a worst-case scenario is when the reference background corresponds to a clear sky and the background behind the chemical cloud corresponds to a mountain. In this condition the two background spectra are quite different and the resulting subtraction residual cannot be simply modelled by a blackbody temperature variation in the fitting process of GASEM. To extend the applicability of our differential detection method to non-uniform background scenarios we are currently developing a background suppression method based on a technique similar to the one proposed by Hayden et al. [2]. This is referred to as the orthogonal background suppression (OBS) technique. The OBS technique removes spatially or temporally varying spectral background structures from the target spectra yielding a spectrally clean signature of the remote chemical vapour cloud. A peculiarity of our approach is that the OBS technique is applied to the differential radiance spectrum rather than to the direct spectrum as proposed in the original method. In this way the probed signal by CATSI benefits from two levels of background suppression, i.e. the suppression by optical subtraction (hardware level) coupled with the OBS technique (software level).

The OBS technique is based on the assumption that the background spectral clutter can be modeled by a linear combination of background spectra taken with no chemical vapour cloud in the field of view [2]. In practice a set of clear background spectra (no cloud) is recorded and compiled in the form of a matrix.

## Military Application of Differential FTIR Radiometry for Passive Standoff Detection

---

The application of singular value decomposition (SVD) to this background matrix yields the orthogonal linear components of the background clutter. Through simple matrix calculations, these components can then be removed from the target spectrum yielding a clean chemical vapour signature. These components can also serve to construct a digital filter for detecting a specific target gas. When applied to the measured spectrum, this filter suppresses the background component and yields the so-called density-contrast product (DCP, see Ref. 2) of the chemical vapour of interest. The units of DCP are column density times radiance ( $CL - \text{Watts/cm}^2\text{-sr-cm}^{-1}$ ).

To describe our initial effort in adapting the OBS technique to the differential detection method with CATSI we have chosen a dataset of measured spectra obtained at a recent field trial held in June 2005 at the Defence Science and Technology Laboratory (DSTL) at Porton Down, UK. One basic experiment performed at this trial was to detect chemical vapour releases at a standoff distance of approximately 500 m for near horizontal path scenarios. In this case the background scene was a mixture of sand, grass and small bushes. This type of background coupled to the environmental and meteorological conditions usually yielded difficult detection conditions due to the low target-to-background radiative contrast. Figure 8A displays one differential radiance spectrum of a temporal sequence recorded during a release of dimethylmethylphosphonate (DMMP). DMMP is a low toxicity chemical agent simulant similar in composition to sarin and is often used to test the performances of passive standoff sensors. The three characteristic spectral bands near 815, 915 and 1050  $\text{cm}^{-1}$  indicates the presence of DMMP. Also shown in Figure 8A is an important positive offset of the differential radiance spectrum in the atmospheric window between 700  $\text{cm}^{-1}$  and 1200  $\text{cm}^{-1}$ . This offset originates from the difference between the two background emission sources (on and off the chemical cloud) simultaneously probed and subtracted by the CATSI sensor. This spectral background residual is mainly caused by the non-homogeneity of the terrain relative to the two fields of view of the CATSI instrument. Figure 8B is a color plot of the full temporal sequence of the differential radiance spectra recorded with CATSI prior to, during and after the DMMP release. In this plot (Fig. 8B) the differential radiance magnitude is color-coded according to the scale on the right side of the plot, and the wavenumber and the measurement time appear on the vertical and the horizontal axis, respectively.

Inspection of Fig. 8B also indicates that the spectral background residual was highly variable during the overall sequence of recording from 0 to 250 seconds. During this sequence, the CATSI sensor was manually operated to sweep different part of the terrain to find the location of the gas release. This contributed to further increase the background residual variability. The release of DMMP began approximately 125 seconds after the spectral acquisition started and last for approximately 100 seconds. Because of the high background residual variability the spectral signature of DMMP is almost undistinguishable in the color-coded spectral sequence of Fig. 8B. In order to apply the OBS technique on these CATSI data we have selected the spectra recorded prior to and after the DMMP release started ( $< 125$  and  $> 225$  seconds). These spectra served as the background database to construct the orthogonal basis vector intervening in OBS and DCP calculations. Figure 8C shows the result of the DCP calculation applied to the full temporal sequence of the spectral acquisition. It is evident that the detection of DMMP based on the DCP is quite efficient. Assuming a gas-to-background thermal contrast of approximately 1 K ( $10^{-7} \text{ Watts/cm}^2\text{-sr-cm}^{-1}$ ) it is found that the maximum column density of the detected DMMP appearing near 160 s is roughly 100 ppm-m. Although this result has not yet been compared to ground-truth data, an estimate of the column density derived from GASEM calculations performed for selected spectra with small offset agree well with the DCP result. Figure 8D represents the full temporal sequence of the recorded spectra after application of OBS processing. A comparison of Figs. 8B and 8D illustrates well the efficiency of the OBS technique to suppress the highly variable background residual components of the CATSI data. For instance the three main spectral bands of DMMP (near 815, 915 and 1050  $\text{cm}^{-1}$ ) show significantly more contrast in the color-coded spectra (Fig. 8D) obtained after OBS application. This encouraging result motivates further development of the OBS technique for processing CATSI data.

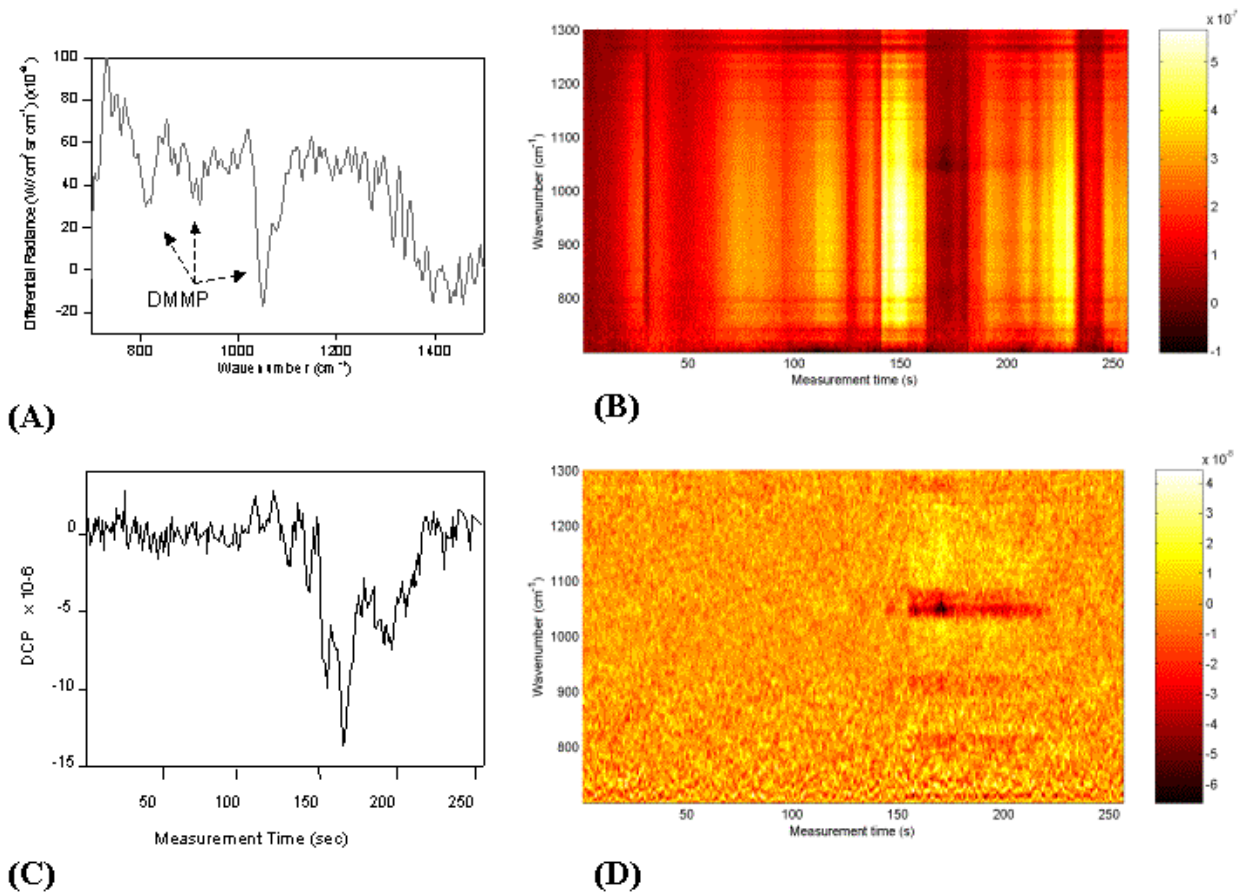


Figure 8: (A) displays a differential radiance spectrum of a temporal sequence recorded during a release of dimethylmethylphosphonate (DMMP); (B) is a colour plot of a temporal sequence of the differential radiance spectra recorded with CATSI; (C) shows the result of the DCP calculation applied to the full temporal sequence of spectrum acquisition; (D) is the full temporal sequence of the recorded spectra after application of OBS processing.

## 6.0 SUMMARY AND CONCLUSION

For the past six years DRDC Valcartier has been developing a method for passive remote sensing by differential Fourier-transform infrared (FTIR) radiometry. The originality of this method lies in the use of a double-input beam FTIR spectrometer (CATSI) optimized for optical subtraction. An overview of the main experimental results obtained at several field trials during the CATSI project development has been presented which clearly demonstrates the successful passive standoff detection of a number of chemical vapours at short (100 m), medium (1.5 km) and long ranges (5.7 km). In addition to chemical vapour detection, the passive standoff detection of liquid contaminants on surfaces was also tested, with encouraging results, at the SURFCON trial (DRDC Suffield, Canada) held in 2002. As well, the passive standoff detection of BG aerosols at ranges of up to 3 km was demonstrated with CATSI at the international TRE trial (Dugway Proving Ground, 2002). Currently, the application of the OBS technique to some recent field measurements obtained at Porton Down, UK, is showing some promise in further reducing the clutter-to-signal ratio of measurements. The peculiarity of our approach is that the OBS technique is applied to the differential radiance spectrum rather than to the direct spectrum as proposed in

## Military Application of Differential FTIR Radiometry for Passive Standoff Detection

---

the original method. In this way the probed signal by CATSI benefits from two levels of background suppression, i.e. the suppression by optical subtraction (hardware level) coupled with the OBS technique (software level).

This work clearly shows the relevance and potential of the differential detection technique for the on-line monitoring and surveillance of toxic chemical agents.

### 7.0 REFERENCES

- [1] D. S. Flanigan, *Prediction of the Limits of Detection of Hazardous vapors by Passive Infrared with the use of MODTRAN*, Appl. Opt., **35**, 6090-6098 (1996).
- [2] A. Hayden, E. Niple and B. Boyce, *Determination of Trace-gas Amounts in Plumes by the use of Orthogonal Digital Filtering of Thermal-emission Spectra*, Appl. Opt., **35**, 2802-2809 (1996).
- [3] J.-M. Thériault, *Modeling the Responsivity and Self-emission of a Double-beam Fourier-transform infrared interferometer*, Appl. Opt., **38**, 505-515 (1999).
- [4] J.-M. Thériault, *Fourier-Transform Spectrometer Configuration Optimized for Self Emission Suppression and Simplified Radiometric Calibration*, United States Patent No. **US 6,233,054 B1**, (May 15, 2001).
- [5] J.-M. Thériault, E. Puckrin, F. Bouffard and B. Déry, *Passive Remote Monitoring of Chemical Vapors by Differential FTIR Radiometry: Results at a Range of 1.5 km*, Appl. Opt., **43**, 1425-1434 (2004).
- [6] J.-M. Thériault, *Passive Standoff Detection of Chemical Vapors by Differential FTIR Radiometry*, DREV Technical Report TR-2000-156 (2001).
- [7] A. Berk, L. S. Bernstein and D. C. Robertson, MODTRAN: A Moderate Resolution Model for LOWTRAN7, *Rpt. No. GL-TR-89-0122*, Air Force Geophys. Lab., Bedford, MA 01731, pp 1-38 (1989).
- [8] C. T. Jr. Chaffin and T. L. Marshall, *Generating Well-Characterized Chemical Plumes for Remote Sensing Research*, in *Electro-optical Technology for Remote Chemical Detection and Identification III*, Mahmoud Fallahi, Ellen Howden, Editors, Proc. SPIE Vol. 3383, 113-123 (1998).
- [9] H. Lavoie, E. Puckrin, J.-M. Thériault and F. Bouffard, *Passive Standoff Detection of SF<sub>6</sub> at a Distance of 5.7 km by Differential FTIR Radiometry*, Vol. 59, Number 10, (2005).
- [10] J.-M. Thériault, E. Puckrin, J. Hancock, P. Lecavalier, C. Jackson Lepage and J.O. Jensen, *Passive Standoff Detection of Chemical Warfare Agents on Surfaces*, Appl. Opt., **43**, 5870-5885 (2004).
- [11] J.-M. Thériault, E. Puckrin and J.O. Jensen, *Passive Standoff Detection of BG Aerosol by FTIR radiometry*, Appl. Opt., **42**, 6696-6705 (2003).